Stem Cell Research & Therapy

RESEARCH

Open Access

# iPSC-derived megakaryocytes and platelets accelerate wound healing and angiogenesis

Kentaro Kosaka[1*], Naoya Takayama[2], Sudip Kumar Paul[2], Maria Alejandra Kanashiro[2], Motohiko Oshima[3], Masaki Fukuyo[4], Bahityar Rahmutulla[4], Ikuko Tajiri[5], Michiaki Mukai[5], Yoshitaka Kubota[1], Shinsuke Akita[1], Nobutaka Furuyama[6], Atsushi Kaneda[4,7], Atsushi Iwama[3], Koji Eto[2,8*] and Nobuyuki Mitsukawa[1*]

## Abstract

**Background** Platelet-rich plasma (PRP), which is prepared by concentrating platelets in autologous blood, shows efficacy in chronic skin wounds via multiple growth factors. However, it exhibits heterogeneity across patients, leading to unstable therapeutic efficacy. Human induced pluripotent stem cell (iPSC)-derived megakaryocytes and platelets (iMPs) are capable of providing a stable supply, holding promise as materials for novel platelet concentrate-based therapies. In this context, we evaluated the effect of iMPs on wound healing and validated lyophilization for clinical applications.

**Methods** The growth factors released by activated iMPs were measured. The effect of the administration of iMPs on human fibroblasts and human umbilical vein endothelial cells (HUVECs) was investigated in vitro. iMPs were applied to dorsal skin defects of diabetic mice to assess the wound closure rate and quantify collagen deposition and angiogenesis. Following the storage of freeze-dried iMPs (FD-iMPs) for three months, the stability of growth factors and their efficacy in animal models were determined.

**Result** Multiple growth factors that promote wound healing were detected in activated iMPs. iMPs specifically released FGF2 and exhibited a superior enhancement of HUVEC proliferation compared to PRP. Moreover, an RNA-seq analysis revealed that iMPs induce polarization to stalk cells and enhance *ANGPTL4* gene expression in HUVECs. Animal studies demonstrated that iMPs promoted wound closure and angiogenesis in chronic wounds caused by diabetes. We also confirmed the long-term stability of growth factors in FD-iMPs and their comparable effects to those of original iMPs in the animal model.

**Conclusion** Our study demonstrates that iMPs promote angiogenesis and wound healing through the activation of vascular endothelial cells. iMPs exhibited more effectiveness than PRP, an effect attributed to the exclusive presence of specific factors including FGF2. Lyophilization enabled the long-term maintenance of the composition of the growth

*Correspondence:
Kentaro Kosaka
knt.k-6098@hotmail.co.jp
Koji Eto
kojieto@cira.kyoto-u.ac.jp
Nobuyuki Mitsukawa
nmitsu@faculty.chiba-u.jp

Full list of author information is available at the end of the article

factors and efficacy of the iMPs, therefore contributing to stable supply for clinical application. These findings suggest that iMPs provide a novel treatment for chronic wounds.

**Keywords** Immortalized megakaryocyte cell lines, Platelets, Wound healing, Growth factors, Lyophilization

## Background

Chronic wounds are those that have failed to progress through an orderly and timely sequence of repair. They can damage the quality of life as severely as kidney or heart failure [1], and their mortality rate is comparable to that of cancer patients [2]. An estimated excess of US$25 billion is spent annually on the treatment of chronic wounds, and the burden is rapidly growing due to aging populations and a sharp rise in the incidence of diabetes and other underlying health conditions worldwide [3]. Therefore, the development of more efficient treatments for chronic wounds is required.

Immediately after skin injury, the contraction of damaged blood vessels and platelets contribute to hemostasis and coagulation. Neutrophils and monocytes are recruited into the wound, triggering an immune response and inflammation. In the following proliferative phase, fibroblasts produce collagen and other extracellular matrix components, and vascular endothelial cells are activated to develop angiogenesis. In the healthy healing process of an acute wound, these cells stimulate each other via cytokines and other factors. However, in a pathological environment, sustained inflammation prevents a smooth progression to the proliferative phase, and cell-cell communication does not operate properly, resulting in chronic wounds [4].

The effects of growth factors, including platelet-derived growth factor-BB (PDGF-BB) [5], fibroblast growth factor 2 (FGF2) [6] and vascular endothelial growth factor (VEGF) [7], on chronic wounds have been confirmed in randomized studies, and these factors have been applied clinically. Nevertheless, in an environment where so many factors are deficient and dysregulated, simply replacing one does not rescue the chronic wound phenotype [8]. In contrast, platelet-rich plasma (PRP), which describes the concentration of platelets from autologous blood of the patient, contains multiple factors that can create an appropriate environment for wound healing [9]. However, despite its general adaptation due to its high efficacy and safety, PRP has several problems. One is heterogeneity of the components across patients, such as a reduced concentration of some growth factors with age [10], which may cause unstable therapeutic efficacy. While leukocytes contained in PRP have been reported to increase efficacy [11], they also induce inflammatory cytokines, which may inhibit wound healing [12]. Moreover, some contraindications of PRP treatment, such as anemia, thrombocytopenia, hemodynamic instability, severe hypovolemia, unstable angina, and sepsis are reported [13].

We have previously reported the induction of megakaryocytes from human induced pluripotent stem cells (iPSCs) and the generation of immortalized megakaryocyte cell lines (imMKCLs) by the transfection of the genes *c-MYC*, *BMI1* and *BCL-XL* [14, 15]. We also found that turbulence plays an essential role in the differentiation of megakaryocytes and have established a unique technique for generating large quantities of platelets from imMKCLs [16]. In comparison with PRP, these resources have the advantage of an abundant supply due to the self-replication potency of imMKCLs and the uniformity of the components independent of the patient. In the present study, we evaluate the efficacy of imMKCLs and their induced platelets (together known as iMPs) as expected novel treatments for chronic wounds and an alternative to standard PRP. In addition, since stability in long-term storage and transport is required for future industrialization, we also validate the lyophilization of these cells, referring to previous reports that freeze-dried PRP show similar efficacy as the original PRP prior to freezing [17].

## Methods

### iMPs preparation

imMKCLs (cell line 7) were cultured as previously reported [15] in Iscove's modified Dulbecco medium (IMDM; Sigma-Aldrich) containing 15% fetal bovine serum (FBS; Nichirei Bioscience), 1 μL/mL L-ascorbic acid (cat. #A4544, Sigma-Aldrich); 1 μL/mL 1-thioglycerol (cat. #M6145, Sigma- Aldrich); a 1% cocktail of 12,000 units/mL penicillin, 10 mg/mL of streptomycin, and 200 mM L-glutamine (cat. #10378-016, Thermo Fisher Scientific); and a 1% cocktail of 1 mg/mL human insulin, 0.55 mg/mL human transferrin, and 0.67 μg/mL sodium selenite (cat. #41400-045, Thermo Fisher Scientific) in the presence of 50 ng/mL human stem cell factor (SCF; cat. #193-15513, FUJIFILM Wako Pure Chemical) and 200 ng/mL TA316 (human thrombopoietin mimetic small compound; in-house synthesized) at 37℃ and 5% $CO_2$. During the proliferation phase of 14 to 50 days, 100 μg/mL doxycycline (Dox; Clontech) was added to the medium to maintain *c-MYC*, *BMI1*, and *BCL-XL* overexpression.

In the differentiation induction phase, Dox was excluded from the medium, and 750 μM SR1 (aryl hydrocarbon receptor antagonist; NARD Institute), 10 mM Y27632 (Rho-associated protein kinase inhibitor; FUJIFILM Wako Pure Chemical), and 15 mM KP457 (inhibitor

of GPIbα shedding on platelets; Kaken Pharmaceutical) were added. $1.0\times10^5$ imMKCLs/mL were incubated in 125-mL Erlenmeyer cell culture flasks shaken by Lab-Therm shakers (Kuhner) to generate shear stress. After incubating for 5 days, the culture medium was centrifuged at 700 x *g* for 15 min, and the cell pellet was suspended in phosphate-buffered saline (PBS) at 1% volume of the medium to collect iMPs.

#### PRP preparation

PRP was extracted from healthy male donors aged 37 to 47 years using a commercial kit (Condensia, Kyocera) according to the instruction manual. Blood containing 5% sodium citrate (Citramin, Fuso Pharmaceutical Industries) was centrifuged at 600 x *g* for 7 min, and the plasma layer with buffy coat was collected. Following the second centrifugation at 2000 x *g* for 5 min, about 80% of the total volume of the supernatant was collected as platelet-poor plasma (PPP), and the remaining layer containing the cell pellet was stirred to acquire PRP. The blood cell densities of whole blood, PPP, and PRP were measured with an automated hematology analyzer (XQ-320, Sysmex). The platelet concentration of PRP was adjusted to five times that of whole blood by adding the calculated amount of PPP.

#### Measurement of cytokines

To activate platelets, 100 U/mL thrombin (Fuji Pharma) was added to the iMPs and PRP, and then both were incubated in a thermostatic chamber at 37 °C for 60 min. Following the activation, the iMPs and PRP were centrifuged at 2000 x *g* for 15 min to collect supernatant containing proteins secreted from the cells. The expression levels of cytokines, including PDGF-BB, transforming growth factor beta (TGF-β), epidermal growth factor (EGF), FGF2, VEGF, and insulin-like growth factor 1 (IGF1), were quantified by an enzyme-linked immuno sorbent assay (ELISA) kit (Quantikine, R&D Systems). All assays were conducted according to the manufacturer's instructions.

#### Cell culture

Human skin fibroblasts derived from adult donors (cat. #CC-2511, Lonza) and HUVECs derived from normal neonate (cat. #C2517A, Lonza) were preliminarily cultured in the manufacturer's recommended growth medium (LONZA) at 37℃ and 5% $CO_2$. To evaluate the paracrine effects of iMPs and PRP in the wound environment, the horizontal co-culture system NICO-1 (Ginrei Lab) was used for in vitro assays. In this system, a filter of 0.6 μm (ICCP filter, Ginrei Lab) is inserted between two linked wells through which proteins, amino acids, and extracellular vesicles can pass [18]. $1\times10^4$ fibroblasts or HUVECs were seeded in one well of NICO-1 and incubated for 24 h. After rinsing with PBS, the culture medium was changed to basal medium. Serum-free Dulbecco's modified Eagle medium (DMEM; Nacalai Tesque) was used as basal medium for the fibroblasts. To prevent excessive apoptosis, DMEM / Ham's F-12 (FUJIFILM Wako Pure Chemical) containing 10% FBS (Life Science Group) was prepared as basal medium for HUVECs. Co-culture was initiated by filling the other well of NICO-1 with basal medium containing 10% iMPs, PRP, or PBS as control and 10 U/mL thrombin.

#### Analysis of proliferation and cell cycle

Following 72 h of co-culture, cells were detached with 0.25% Trypsin-EDTA (FUJIFILM Wako Pure Chemical) and collected for cell counting with a flow cytometer (FACS Canto II, Becton, Dickinson & Co.) and counting beads (cat. #C36950, Thermo Fisher Scientific). The number of fibroblasts in each group was determined after excluding propidium iodide (cat. #00-6990-42, Thermo Fisher Scientific) positive dying cells. A cell cycle assay was performed as previously reported [19]. Briefly, collected cells were fixed and permeabilized in 100 mL of BD Cytofix/Cytoperm (Becton, Dickinson & Co.) for 15 min on ice and then washed in BD Perm/Wash buffer (Becton, Dickinson & Co.). Next, the cells were treated with BD Cytoperm permeabilization buffer Plus (Becton, Dickinson & Co.) for 10 min on ice, washed in BD Perm/Wash buffer, and incubated in BD Cytofix/Cytoperm for 5 min on ice. After another wash with BD Perm/Wash, the cells were stained with Ki67-Alexa647 (cat. #558615, Becton, Dickinson & Co.) at 4 °C overnight (dilution 1:30 in BD Perm/Wash buffer). The cells were then washed with BD Perm/Wash and incubated with 7AAD (cat. #559925, Becton, Dickinson & Co.) at 1:40 dilution for 20 min at room temperature. Finally, the cells were analyzed with a flow cytometer within an hour.

#### Evaluation of FGF2 function on HUVEC proliferation

To verify the effect of FGF2 contained in iMPs on HUVECs, 1.5 or 10 ng/mL recombinant FGF2 (cat. #ab9596, Abcam) was added to the basal medium instead of the co-culture. After 72 h of incubation, the number of HUVECs was determined with a flow cytometer, as described above. In addition, 2 nM of an FGFR inhibitor, Pemigatinib (cat. #S0088, Selleck) or Futibatinib (cat. #S8848, Selleck), was added to the basal medium at the initiation of the co-culture with iMPs. Dimethyl sulfoxide (DMSO) was used as the inhibitor solvent and control. The number of HUVECs was determined after 72 h.

#### RT-qPCR

Total RNA was extracted from fibroblasts or HUVECs using the RNeasy Micro Kit (Qiagen) and reverse transcribed using the ReverTra Ace qPCR RT Master Mix Kit (Toyobo). Synthesized cDNA was subjected to

quantitative reverse transcription polymerase chain reaction (RT-qPCR) with TaqMan Gene Expression Master Mix (Thermo Fisher Scientific) using CFX Connect (Bio-Rad). Amplification was performed using specific primers (cat. #4331182, Thermo Fisher Scientific). The analyzed genes and their primer ID were *GAPDH* (Hs02786624_g1), *ACTA2* (Hs00426835_g1), *FGF2* (Hs00266645_m1), *VEGF* (Hs00900055_m1). Gene expressions were quantified as the relative mRNA level normalized to *GAPDH*.

#### Transwell migration assay

HUVEC migration was analyzed using a transwell with an 8.0-μm pore membrane insert (Corning). The lower chamber contained 2.5 mL basal medium with 10% iMPs, PRP, or PBS and 10 U/mL thrombin. 100 μL of serum-free DMEM including $5\times10^4$ HUVECs was added to the insert, which was placed on each well of a 24-well plate. After 24 h of incubation, remaining cells on the upper side of the membrane were wiped out with cotton swabs. Then, the cells that penetrated the lower side were fixed with 4% paraformaldehyde phosphate buffer solution (FUJIFILM Wako Pure Chemical) and stained with 1% crystal violet (bioWORLD) for 10 min. The center of the membrane was photographed with a digital phase contrast microscope (BZ-X700, Keyence), and the stained area was quantified using analysis software (BZ-X Analyzer, Keyence).

#### RNA-seq

After 72 h of co-culture, total RNA was extracted from HUVECs using the RNeasy Micro Kit. RNA-seq libraries were prepared from at least three biological replicates according to the manufacturer's protocol. Briefly, ~10 ng total RNA was used as input for cDNA conversion using a SMART-Seq v4 Ultra Low Input RNA Kit for Sequencing (cat. #634890, Clontech, Takara). cDNA was fragmented using an S220 Focused-ultrasonicator (Covaris). The cDNA library was then amplified using a NEBNext Ultra DNA Library Prep Kit for Illumina (cat. #E7370L, New England Biolabs). Finally, the NEBnext library size was estimated using a bioanalyzer with an Agilent High Sensitivity DNA Kit. Sequencing was performed using a NextSeq500 System (Illumina) with a single-read sequencing length of 60 bp. TopHat (version 2.1.1; with default parameters) was used to map to the reference genome (UCSC/hg19) with annotation data from iGenomes (Illumina). Gene expression levels were quantified using Cuffdiff (Cufflinks version 2.2.1; with default parameters).

#### Knockdown of *ANGPTL4*

24 h after seeding HUVECs in NICO-1, siRNA was transfected using Lipofectamine RNAiMAX (cat. #13778030, Thermo Fisher Scientific). The cells were incubated for 6 h in serum-free Opti-MEM (Thermo Fisher Scientific) containing 10 nM of siRNA SMARTpool (cat. #M-007807-02, Dharmacon) or Non-Targeting Control siRNAs (cat. #D-001210-03, Dharmacon). After changing the medium to basal medium, the cells were co-cultured with iMPs or administered 1.5 ng/mL FGF2, as described above. The number of HUVECs in each group was counted after 72 h with a flow cytometer. The knockdown efficiency in HUVECs was evaluated by RT-qPCR 72 h after the transfection.

#### In vivo wound healing assay

8-12-week-old female diabetic mice (BKS.Cg-*m* +/+ *Lepr$^{db}$*/Jcl, CLEA Japan) were prepared for the animal experiments. Anesthesia was performed using isoflurane (Fujifilm Wako Pure Chemical) with an animal anesthetizer device (MK-AT210D, Muromachi Kikai). The concentration of isoflurane was 2% to provide an appropriate depth of anesthesia during the following surgical procedure. After hair removal with shaving and depilatory cream (Veet, Reckitt Japan), full thickness skin defects of 20 mm in diameter were introduced on the center of the back using a scalpel and scissors. The mice were randomly divided into three groups: iMPs, PRP, and PBS as control. 100 μL of each sample and 10 U of thrombin were applied onto the wound surface, and polyurethane film (Tegaderm, 3 M) was placed over the wound. This sample application procedure was also performed on day 3. Mice were placed in individual cages during the experiment. On days 0, 3, 6, 8, 10, 13, 15, 17, and 20, after removing the dressing, the wound was photographed with a digital camera (EOS 80D, Canon). Each non-epithelialized area was calculated using Adobe Photoshop software. At the end of the observation period, the mice were humanely euthanized with carbon dioxide in accordance with the institutional guidelines. All animal experiments were reported in line with the ARRIVE guidelines 2.0.

#### Histological analysis

On day 10 of the wound healing assay described above, mice from each group were euthanized with carbon dioxide for histological analysis. Skin samples, including wounds, were taken and fixed with 10% Formalin Neutral Buffer Solution (Fujifilm Wako Pure Chemical). The samples were embedded in paraffin and sectioned at each wound axially.

Masson's trichrome staining was performed to evaluate collagen formation. Tissue sections were stained in Iron Hematoxylin Working Solution, 0.75% Orange G Staining Solution, Masson's Staining Solution A, and Aniline Blue Solution. All solutions were purchased from Muto Pure Chemicals. Images of the whole section were acquired using a digital microscope (BZ-X700, Keyence) at low

magnification. The area where the loss of hair follicles was observed was identified as the original wound, and the total area of the blue-stained area within the wound was measured using analysis software (BZ-X Analyzer, Keyence).

To quantify angiogenesis in the wound, immunohistochemical staining was performed. Tissue sections were de-paraffined with xylene. Antigen retrieval was performed by microwave treatment with EDTA Buffer (Genostaff). Endogenous peroxidase was blocked with 0.3% $H_2O_2$ in methanol, followed by incubation with G-Block (Genostaff) and an Avidin/Biotin Blocking Kit (Vector Laboratories). The sections were incubated with Anti-CD31 Rabbit Monoclonal Antibody (cat. #ab182981, Abcam) overnight. They were then incubated with Biotin-Conjugated Anti-Rabbit IgG (cat. #BA-1000, Vector Laboratories), followed by the addition of peroxidase conjugated streptavidin (Nichirei). Peroxidase activity was visualized using diaminobenzidine. The sections were counterstained with Mayer's Hematoxylin (Muto Pure Chemicals) and mounted with Malinol (Muto Pure Chemicals). Images were acquired using a digital microscope (BZ-X700, Keyence) at high magnification. The average number of stained blood vessels in 10 random fields of view in each wound was calculated.

#### Validation of FD-iMPs

The iMPs lyophilization procedure was performed using VA-140 S (Taitec). iMPs collected as described above were transferred to a test tube and rotated in an ethanol bath at -60 °C for preliminary freezing. After 24 h of incubation at -80 °C, the tube was attached to a vacuum freeze-dryer to complete the process. Freeze-dried iMPs (FD-iMPs) were stored at 4 °C for 90 days to evaluate their stability and then applied for growth factor measurement by ELISA and for the in vivo wound healing assay. In these experiments, FD-iMPs were previously suspended in PBS to the same volume as before lyophilization.

#### Statistical analysis

All data are represented as means ± SEM and were analyzed using GraphPad Prism 8 (GraphPad Software). Pairwise comparisons were performed using a two-tailed t-test with assumed equal variances. When comparing three or more groups, one-way ANOVA and the Tukey-Kramer test were applied. Conventional statistical significance was set at $p < 0.05$.

## Results

#### Activated iMPs release a different set of growth factors than PRP

PDGF-BB, TGF-β, EGF, FGF2, VEGF [20], and IGF-1 [21] have been reported as cytokines that promote wound healing. Investigation of these growth factors derived from iMPs (Fig. 1A) by ELISA showed similar levels of PDGF and EGF and twice the concentration of TGF-β compared to PRP. FGF2 was not detected in PRP but found to be present in iMPs at a concentration of 32 ng/mL. In contrast, VEGF was present in PRP at a concentration five times higher than that in iMPs, and IGF-1 was specifically detected in PRP but not in iMPs (Fig. 1B). When thrombin was excluded from the activation process, the concentrations of PDGF, TGF, EGF, and FGF2 in iMPs were all significantly decreased (Fig. 1C).

#### iMPs promote fibroblast proliferation and growth factor expression

We assessed the effects of iMPs and PRP on human skin fibroblasts using the horizontal co-culture system (Fig. 2A). Fibroblast proliferation was significantly increased in both groups compared to the control group: 2.0-fold in the iMPs group and 6.9-fold in the PRP group. Thus, PRP demonstrated a higher efficacy than iMPs (Fig. 2B). We also examined the cell cycle status of fibroblasts treated with iMPs and PRP. Since we could not detect a Ki67 positive fibroblast population, only 7AAD was used for the analysis. Both groups exhibited significantly higher rates of 7AAD compared to the control group, indicating accelerated proliferation (Fig. 2C).

To investigate the changes in gene expression induced by iMPs and PRP, RT-qPCR was performed on the collected fibroblasts. The expression of *ACTA2*, a differentiation marker of myofibroblasts [22], was significantly suppressed in both groups. In contrast, iMPs enhanced the gene expression of *FGF2* and *VEGF*, both of which have been reported to be secreted from fibroblasts and contribute to cell-cell interactions in the proliferative phase of wound healing [23] (Fig. 2D). In addition, the proteins released from fibroblasts were quantified. Following the separation of wells to terminate the co-culture, the fibroblasts were incubated in serum-free medium for 24 h. FGF2 and VEGF protein concentrations in the collected medium were measured using ELISA. Consistent with the gene expression, both proteins were increased in the iMPs group compared to the control group (Fig. 2E).

#### iMPs promote vascular endothelial cell proliferation via FGF2

We also evaluated the effect of iMPs on vascular endothelial cells, which play an important role in angiogenesis in wound healing. The proliferative potential of HUVECs was increased 2.2-fold in the PRP group and 17-fold in the iMPs group compared to the control group (Fig. 3A). iMPs showed an 8.8-fold higher efficacy than PRP, which contrasts the results of the fibroblast proliferation assay. Moreover, the iMPs group had a specifically higher proportion of cells in the $G_1$ and $G_2$/M cell cycle phases

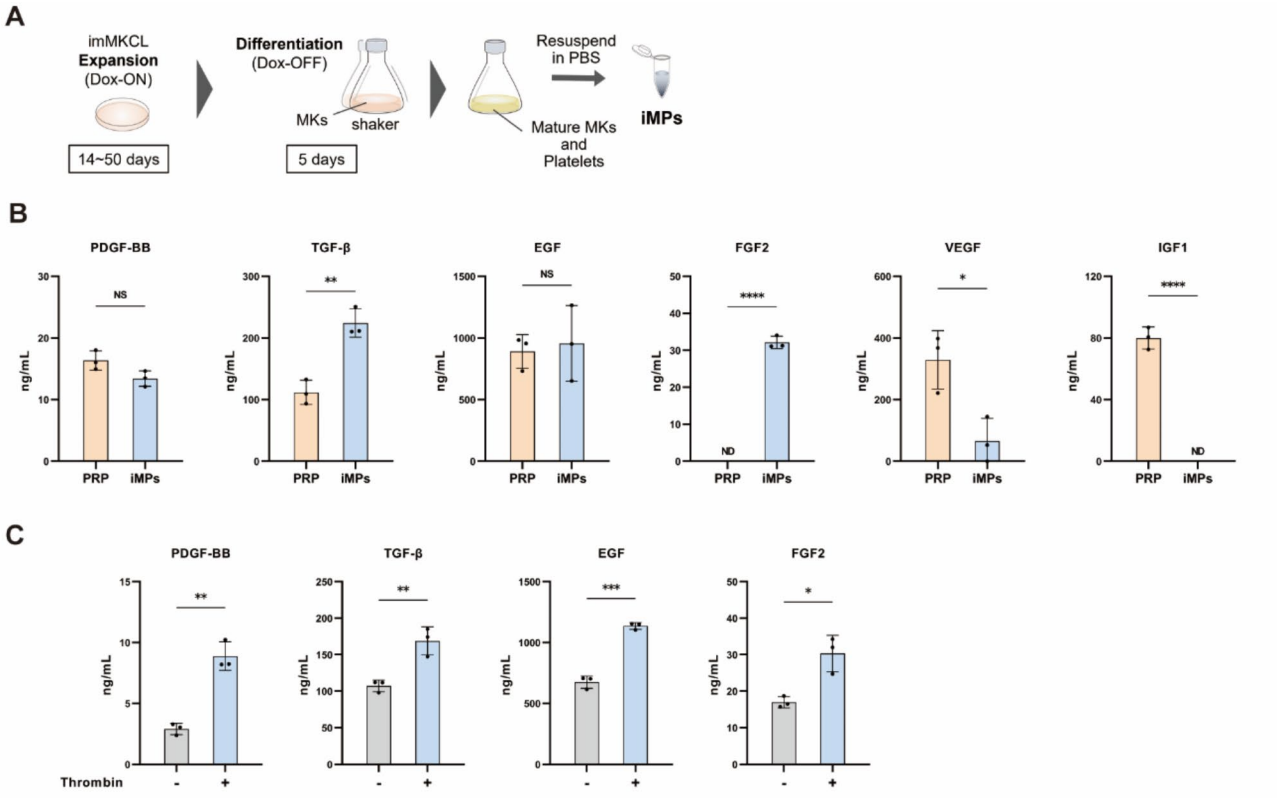


**Fig. 1** Preparation of iMPs and measurement of growth factors. **A** Schema of the preparation. Following 5 days of imMKCL differentiation with DOX removal, a mixture of mature megakaryocytes and platelets were collected as iMPs. **B** Concentration of growth factors in iMPs that have been previously reported to promote wound healing. Following the activation, PDGF-BB, TGF-β, EGF, VEGF, FGF2, and IGF1 in the supernatant were quantified using ELISA. $n = 3$. **C** Thrombin dependency of the growth factors released from iMPs. Their concentrations were determined with and without thrombin during the activation. $n = 3$. Data are presented as the mean ± SD. * $p < 0.05$, ** $p < 0.01$, *** $p < 0.001$, **** $p < 0.0001$. NS: not significant. ND: not detected

compared to the control group (Fig. 3B). In contrast, the transwell assay showed that migration in the PRP group was enhanced 7.1-fold compared to the control group but no change in the iMPs group (Fig. 3C).

We next focused on FGF2, because it was specifically detected in iMPs, and hypothesized that it generated the proliferation difference between the iMPs and PRP groups. HUVEC proliferation was evaluated with the following concentrations of FGF2 added to the culture medium: 1.5 ng/mL, which was calculated to be approximately equal to the concentration in the culture medium of the iMPs group in reference to the ELISA results, and 10 ng/mL, which was reported to be a sufficient concentration for HUVEC growth [24]. At these concentrations, the single treatment of FGF2 promoted the cell proliferation (Fig. 3D). Furthermore, Pemigatinib and Futibatinib partially reduced the effect of iMPs (Fig. 3E). These two drugs selectively inhibit FGFR1-4, the major receptors of FGF2 [25, 26]. Notably, at 1.5 ng/mL FGF2, HUVEC proliferation reached a plateau that was 0.52-fold lower than in the iMPs group.

### iMPs change polarity and upregulate *ANGPTL4* in HUVECs

The above findings suggest that iMPs include unknown factors that promote HUVEC proliferation in addition to FGF2. To identify the mechanism, the gene expressions of HUVECs in each group were analyzed by RNA-seq. Compared to the control group, 420 genes were up-regulated in the PRP group, 501 in the FGF2 group, and 812 in the iMPs group (Fig. 4A). A Gene Set Enrichment Analysis (GSEA) (Table S1) demonstrated a significant enrichment of the cell cycle pathway in the FGF2 and iMPs groups, consistent with the proliferation assay (Fig. 4B, C). In contrast, the collagen formation pathway was enriched in the PRP group only (Fig. 4B, D). A pairwise comparison of the FGF2 and iMPs groups showed that 370 genes were upregulated and 174 genes were downregulated in the iMPs group (Fig. 5A). An analysis of the differentially expressed genes between the two groups using g: profiler [27] revealed that the vascular development pathway was included in the top 10 significantly enriched GO: biological process pathways (Fig. 5B, C, Table S2). Recent studies showed the polarity of endothelial cells in the process of vascular development: motile tip cells and

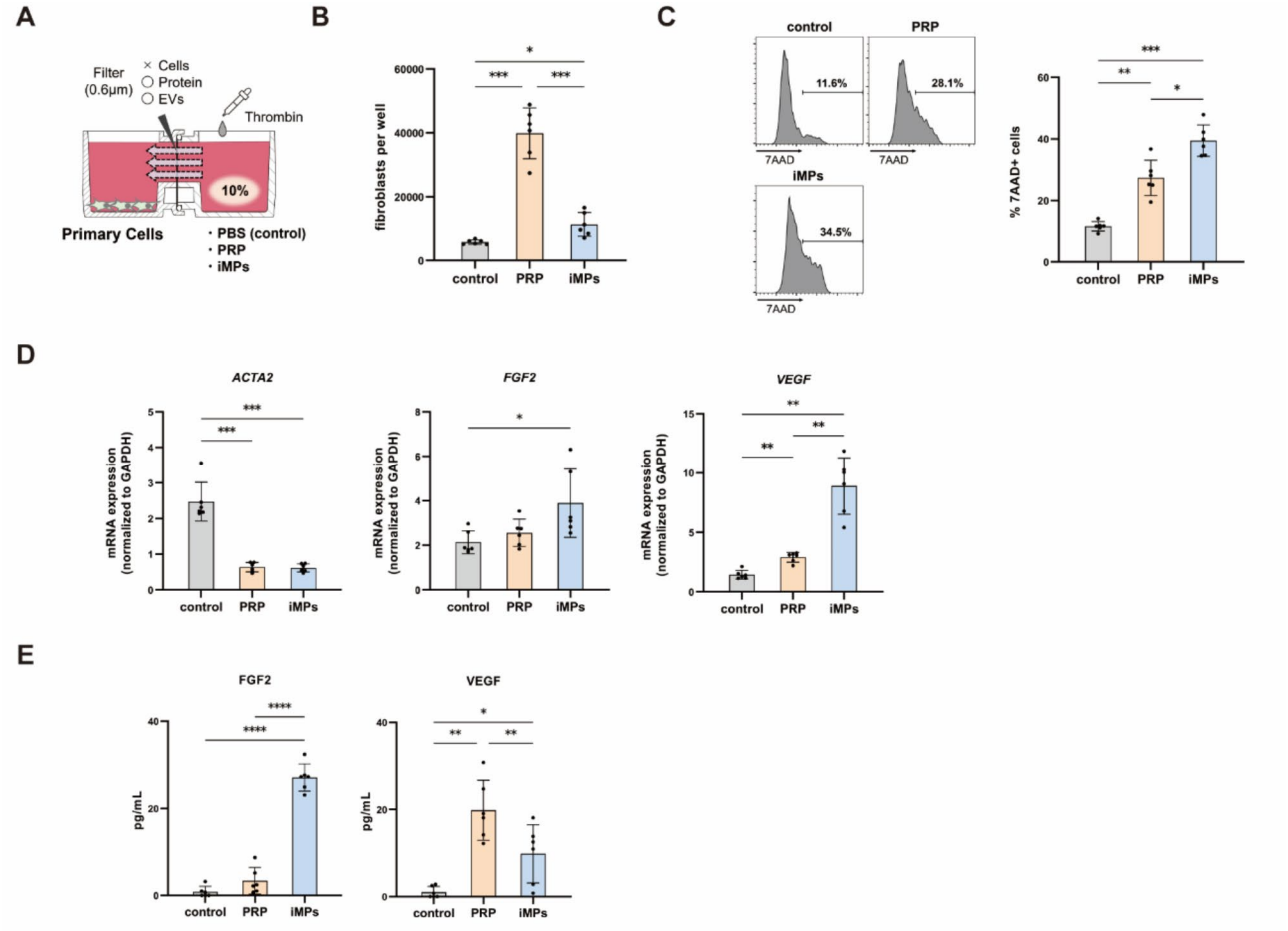


**Fig. 2** Effects of iMPs on fibroblasts in vitro. **A** Shema of the assay using the NICO-1 co-culture system. This system has a filter of 0.6 μm between two linked wells, enabling evaluation of the paracrine effect in a biological wound environment. Primary cells were seeded in one well, while culture medium containing 10% PBS, PRP, or iMPs filled the other well. **B** Fibroblast proliferation. Following 72 h of co-culture, the number of fibroblasts per well was counted. $n=6$. **C** Cell cycle of fibroblasts. Representative plots show 7AAD staining after 72 h of co-culture. The positive rate of 7AAD is indicated in the bar graph. $n=6$. **D** Gene expressions of *ACTA2*, *FGF2*, and *VEGF* in fibroblasts. *ACTA2* is a differentiation marker of myofibroblasts. FGF2 and VEGF are secreted from fibroblasts and contribute to cell-cell interactions in wound healing. $n=6$. **E** Concentrations of FGF2 and VEGF released into the culture medium from fibroblasts following the co-culture. $n=6$. Data are presented as the mean ± SD. * $p<0.05$, ** $p<0.01$, *** $p<0.001$, **** $p<0.0001$

proliferative stalk cells [28]. To understand the contribution of iMPs to the fate decision, the expression of the marker genes of tip cells and stalk cells [29] were compared between the iMPs and FGF2 groups. Five stalk cell marker genes were upregulated in the iMPs group, while 9 tip cell marker genes including DLL4 were upregulated in the FGF2 group (Fig. 5D). Additionally, the proliferation-promoting gene *ANGPTL4* [30] was significantly upregulated in the iMPs group compared to the FGF2 group (Fig. 5E). HUVECs in which *ANGPTL4* gene was knocked down by siRNA had a reduced response to iMPs specifically (Fig. 5F, G). These findings suggest that iMPs enhance the proliferation of endothelial cells by changing polarity and upregulating *ANGPTL4* independently of FGF2 signaling pathways.

### iMPs enhance wound healing in diabetic animal models

Diabetes is one of the most prevalent causes of chronic wounds [31]. To investigate the phenotypic impact of the functional mechanisms of iMPs as revealed by the in vitro assays, iMPs and PRP were applied to defects on the dorsal skin of diabetic mice (Fig. 6A). Both groups exhibited a significantly increased wound closure rate compared to the control group after day 10 of the primary treatment. However, from days 13 to 17, iMPs demonstrated a higher contribution to wound healing compared to PRP (Fig. 6B). A histological analysis showed that a larger amount of collagen was synthesized in the iMPs group compared to the control group (Fig. 6C). Furthermore, significantly more neovessels developed in the iMPs group compared to the PRP group (Fig. 6D), an observation consistent with the findings of the HUVEC proliferation assay.

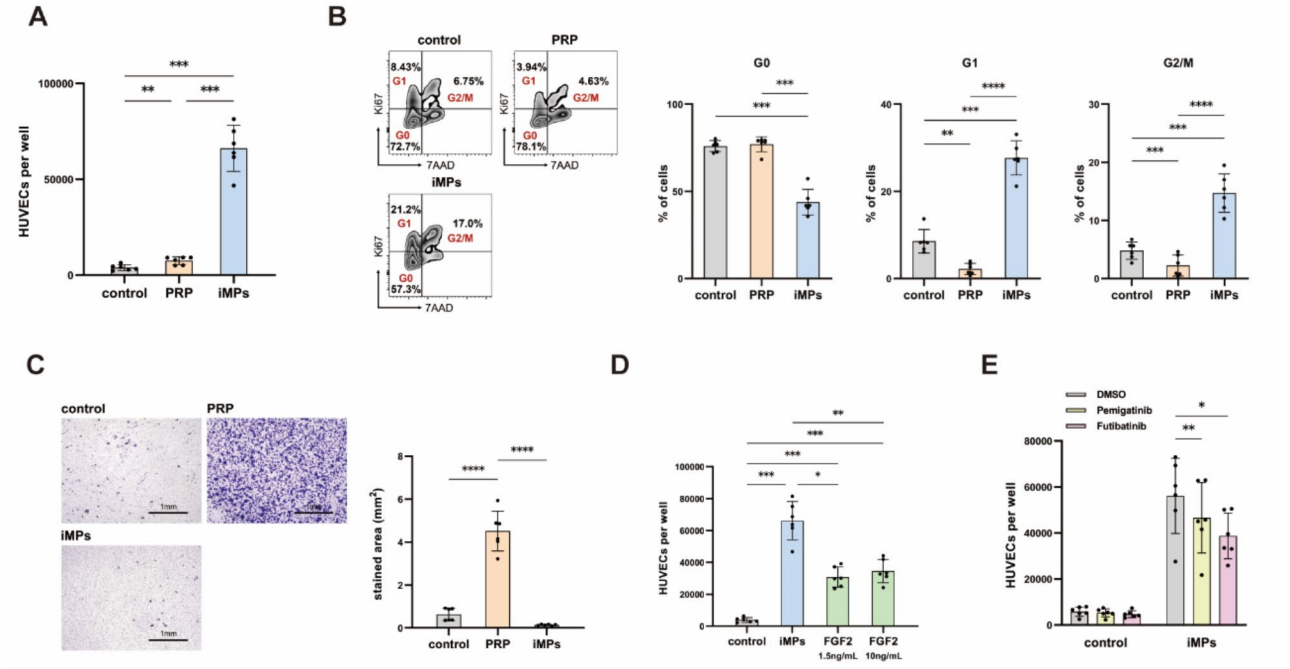


**Fig. 3** Effect of iMPs on vascular endothelial cells in vitro. **A** HUVEC proliferation. Following 72 h of co-culture, the number of HUVECs per well were counted. $n=6$. **B** Cell cycle of HUVECs. Representative plots show 7AAD and Ki67 staining after 72 h of co-culture. $G_0$, 7AAD$^-$Ki67$^-$; $G_1$, 7AAD$^-$Ki67$^+$; $G_2$/M, 7AAD$^+$Ki67$^+$. The percentage of cells in $G_0$, $G_1$, and $G_2$/M is indicated in the bar graphs. $n=6$. **C** Evaluation of HUVEC migration by the transwell assay. Cells that penetrated into the lower side of the membrane, which was placed on the well containing iMPs or PRP, were stained with crystal violet. The calculated area of stained cells is shown in the bar graph. $n=6$. **D** Effect of FGF2 on HUVEC proliferation. 1.5 or 10 ng/mL FGF2 was added to the culture medium, and the cell number was counted after 72 h of incubation. $n=6$. **E** FGFR-inhibition assay. The FGFR inhibitors Pemigatinib and Futibatinib or the control DMSO were administered to HUVECs at the initiation of the co-culture with iMPs. The number of HUVECs was determined after 72 h of co-culture. $n=6$. Data are presented as the mean ± SD. * $p<0.05$, ** $p<0.01$, *** $p<0.001$

### Lyophilization contributes to long-term stability of iMPs

Lastly, we prepared and validated FD-iMPs to optimize iMPs for long-term storage (Fig. 7A). The concentration of growth factors in FD-iMPs following storage for three months was measured by ELISA and compared with the original iMPs. The concentrations of PDGF-BB, TGF-β, EGF, and FGF2 in FD-iMPs were significantly higher compared to the original iMPs. The EGF concentration showed the largest increase (9.3 times) among these factors (Fig. 7B). Meanwhile, the wound closure rate in the animal model was higher in the FD-iMPs group compared to the control group but not significantly different from the original iMPs group (Fig. 7C).

## Discussion

In 1998, Marx et al. first demonstrated the tissue-repairing effects of PRP with grafted bone [32]; this finding was subsequently applied to the treatment of chronic wounds. A recent systematic review showed that the rate of complete closure of chronic wounds by PRP was significantly higher than in untreated patients with an odds ratio of 5.32 [33]. Considering the remarkable effectiveness of PRP but also disadvantages, such as heterogeneity and contraindications, we focused on the potential of imMKCLs and their induced platelets (iMPs) as a novel therapeutic agent. Our findings demonstrated that iMPs accelerate wound healing through the activation of vascular endothelial cells and fibroblasts. Interestingly, this mechanism was found to be partially different from that of PRP, and animal experiments showed a significantly higher efficacy of iMPs.

The variety of cytokines released from α-granules in activated platelets produces an environment conducive to wound healing [4]. We previously reported that imMKCL-derived platelets contain granules similarly to human donor platelets [15]. The finding that multiple growth factors with increasing concentrations in a thrombin-dependent manner were detected in iMPs confirms that they were released from the granules. In a comparison between iMPs and PRP, some of the growth factors demonstrated specific expression levels or significant differences in concentration levels. These discrepancies are presumed to be attributed to the following. First, megakaryocytes are specifically included in iMPs. Since we hypothesized that mature megakaryocytes and platelets are both major resources of wound-healing promoting factors, we utilized iMPs. Second, iPSC-derived cells typically show fetal cell characteristics [34], whereas the primary platelets in PRP were differentiated from megakaryocytes from adult bone marrow. Third, PRP

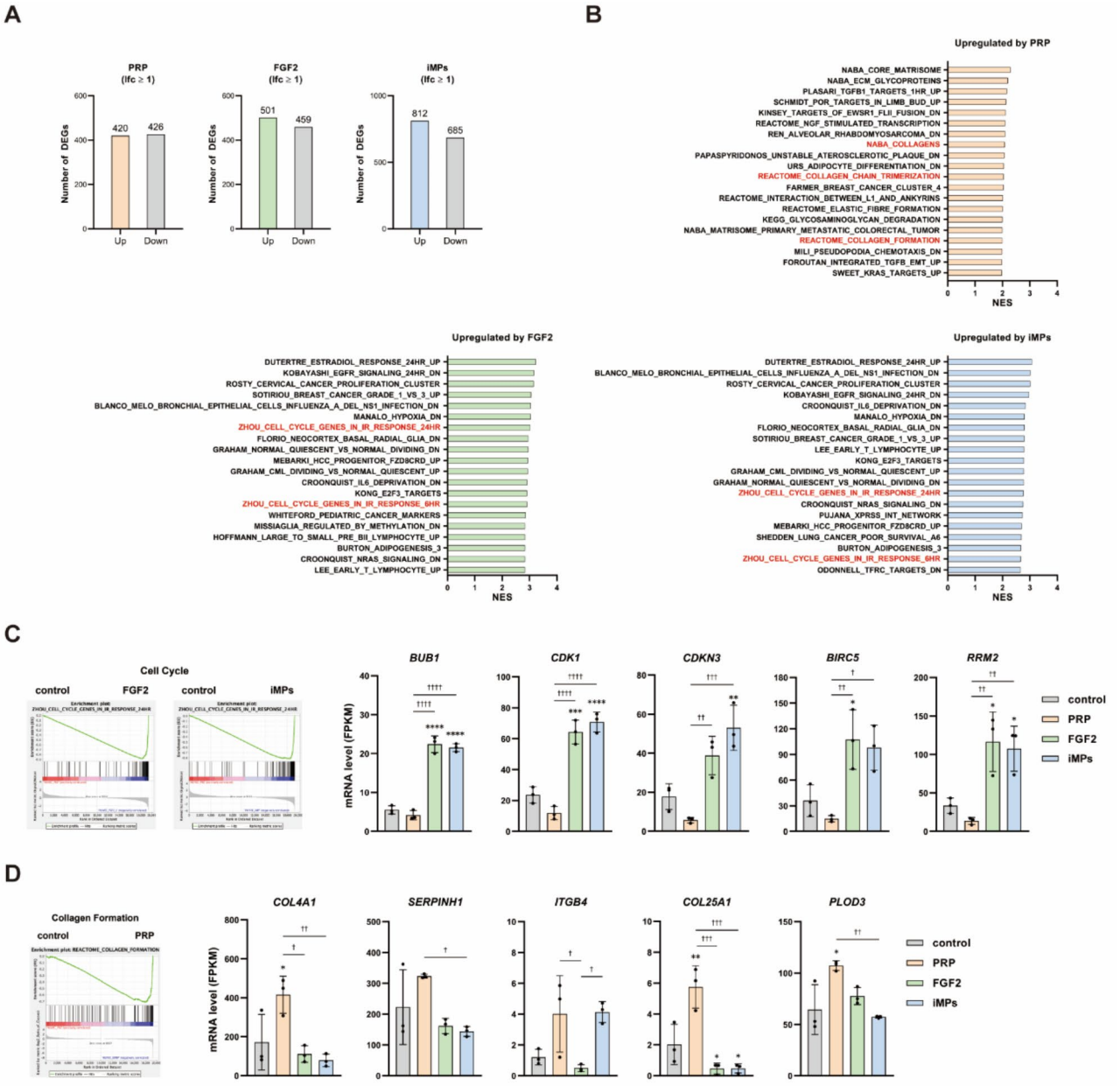


**Fig. 4** Changes in HUVEC gene expressions induced by PRP, FGF2, and iMPs. Total RNA of HUVECs in each group was extracted for RNA-seq following the co-culture described in Fig. 3. $n = 3$. **A** The number of differentially expressed genes (DEGs) compared with the control group. **B** The top 20 most significantly upregulated pathways in the GSEA. The respective normalized enrichment score (NES) is indicated in the bar graphs. The overall data is available in supplementary table S1. **C** Enrichment of the cell cycle pathway in the iMPs and FGF2 groups. **D** Enrichment of the collagen formation pathway in the PRP group. In **C** and **D**, the fragments per kilobase of exon per million reads mapped (FPKM) of individual genes included in the gene sets is indicated. Data are presented as the mean ± SD. * $p < 0.05$, ** $p < 0.01$, *** $p < 0.001$, **** $p < 0.0001$ versus the control group. † $p < 0.05$, †† $p < 0.01$, ††† $p < 0.001$, †††† $p < 0.0001$

specifically contain plasma and leukocytes, which are possible sources of growth factors not included in iMPs.

The distinct differences in the effects of iMPs and PRP on primary cells associated with wound healing in vitro were the result of discrepancies in their components. iMPs specifically contained FGF2, which is known to promote angiogenesis and contribute to the healing of chronic wounds [35]. Accordingly, iMPs exhibited a superior effect on HUVEC proliferation compared to PRP, a difference that was partially reproduced by the administration of FGF2. Furthermore, the effect of iMPs was suppressed by FGF2 inhibitors. These results suggest that FGF2 is one of the mechanisms by which iMPs support vascular endothelial cell proliferation. However, iMPs showed an approximately 1.9-fold effect compared to FGF2. The pairwise comparison of gene expressions

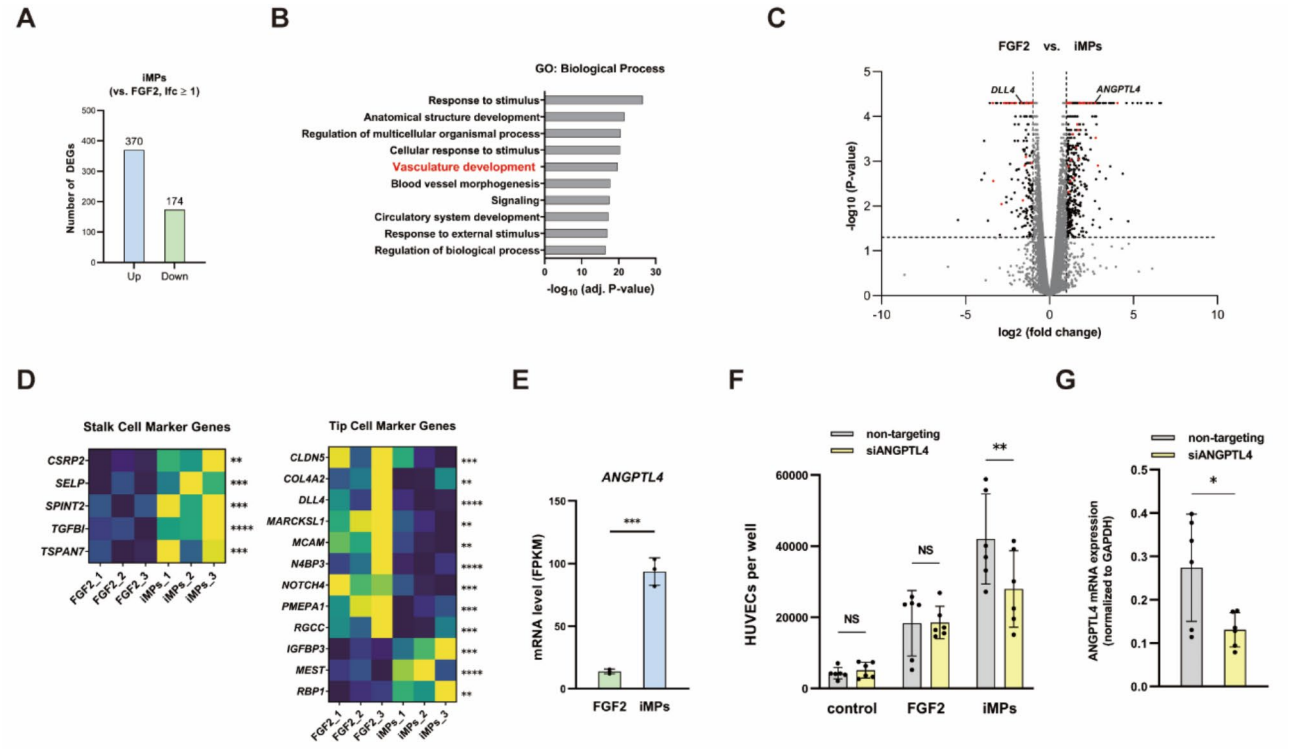


**Fig. 5** Pairwise comparison of HUVEC gene expressions between the FGF2 and iMPs groups. **A** The number of differentially expressed genes (DEGs) in the iMPs group in comparison with the FGF2 group. **B** Pathways detected using g: profiler. Both upregulated and downregulated genes in the iMPs group compared to the FGF2 group were analyzed with g: profiler. The top 10 most significantly enriched pathways included in the GO: biological process are shown. All enriched pathways are available in supplementary table S2. **C** A volcano plot of individual genes in both groups. Significantly upregulated or downregulated genes that are included in the vascular development pathway are indicated as red dots. **D** Expressions of genes related to the polarity of endothelial cells. Marker genes of stalk cells and tip cells that showed significantly different expression between the two groups are represented in the heatmaps. The fragments per kilobase of exon per million reads mapped (FPKM) values were used to generate the heatmaps. ** $p < 0.01$, *** $p < 0.001$, **** $p < 0.0001$. **E** Expression of *ANGPTL4* gene in the two groups. $n = 3$. **F** Knockdown of *ANGPTL4*. siANGPTL4 or non-targeting control siRNA was transfected into HUVECs. Afterwards, the cells were co-cultured with iMPs or administered FGF2. The number of HUVECs in each group was counted after 72 h. $n = 6$. **G** Knockdown efficiency of siRNA. The expression of *ANGPTL4* in HUVECs was evaluated by RT-qPCR 72 h after the transfection. Three independent experiments were performed in technical duplicate. Data are presented as the mean ± SD. * $p < 0.05$, ** $p < 0.01$, *** $p < 0.001$. NS: not significant

in HUVECs based on the RNA-seq analysis revealed that different polarities were induced: tip cell-related genes in the FGF2 group and stalk cell-related genes in the iMPs group were upregulated. During angiogenesis, motile tip cells lead and guide endothelial sprouts, while proliferative stalk cells trailing tip cells elongate the sprouts and form lumens. These phenotypes regulated by the DLL4-NOTCH signal are transient and exchangeable [29]. Our findings that iMPs promote the proliferation but not migration of HUVECs are consistent with the polarity transition from tip cells to stalk cells. Moreover, *ANGPTL4* was significantly upregulated by iMPs compared to FGF2. A recent study revealed that *ANGPTL4* accelerates the proliferation of primary vascular endothelial cells [30]. That the transfection of siANGPTL4 in HUVECs reduced the effect of iMPs specifically implies that upregulation of *ANGPTL4* is a mechanism that promotes proliferation in an FGF2-independent manner. Overall, our findings suggest that iMPs enhance the proliferative potential of endothelial cells by inducing differentiation into stalk cells and upregulating *ANGPTL4*. The stimulating factors of these signals included in iMPs will be identified in future research. The proliferation assays of fibroblasts demonstrated superior effects in the PRP group compared to the iMPs group, which contrasts the observations of HUVECs. However, the enhanced FGF2 and VEGF expression in fibroblasts suggests that iMPs activate vascular endothelial cells through a paracrine effect from fibroblasts in addition to their direct effect. Therefore, the main target cells of iMPs and PRP and their mechanism in wound healing are different.

Peripheral vascular dysfunction is one of the pathologies of diabetic skin ulcers [31]. The chronic wound model was developed in diabetic mice that have a mutation in the leptin receptor [36–38]. The observations that iMPs significantly accelerated wound healing and increased neovascularity compared to PRP in the animal model are consistent with the findings of the in vitro assays and support the clinical efficacy of iMPs. However, the phenotypic relevance of the different outcomes

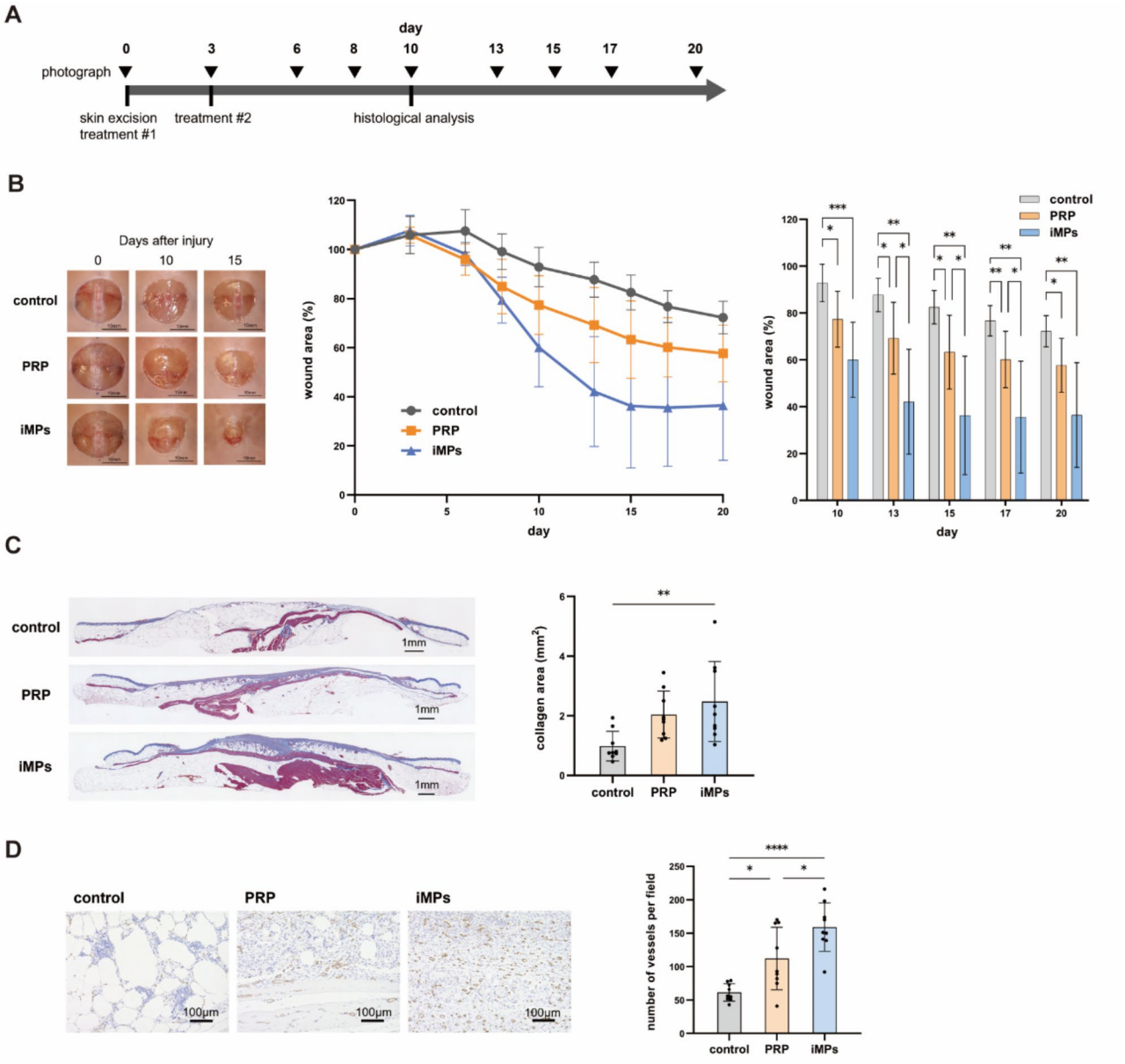


**Fig. 6** Effectiveness of iMPs in wound healing of mouse skin. **A** Schematic illustration representing the in vivo assay using a diabetic mouse model. Full thickness skin defects of 20 mm in diameter were introduced on the back. On days 0 and 3, PBS, PRP, or iMPs was applied onto the wound surface. Until day 20, the wound was photographed, and the non-epithelialized area was calculated. Histological analysis was performed on day 10. **B** Chronological analysis of the wound closure rate. Representative images of each group are presented. Statistical differences on days 10 to 20 are indicated in the bar graph. $n = 9$. **C** Evaluation of collagen formation with Masson's trichrome staining. The area where the loss of hair follicles was observed was identified as the original wound, and the total area of the blue-stained area within the wound was measured using analysis software. $n = 9$. **D** Evaluation of angiogenesis with immunohistochemical staining for CD31. High magnification images were taken at 10 random fields of view within the wound. The average number of stained blood vessels was calculated using analysis software. $n = 9$. Data are presented as the mean ± SD. * $p < 0.05$, ** $p < 0.01$, *** $p < 0.001$, **** $p < 0.0001$

between iMPs and PRP, such as fibroblast proliferation and the expression of collagen synthesis genes in HUVECs, including *COL4A1*, which is a crucial factor for the formation of basement membranes, needs further investigation.

Our finding that lyophilization increases the amount of growth factors derived from iMPs has been similarly reported for PRP [17]. This outcome is presumed to be caused by the mechanical crushing of platelets and exhaustive release of granules. The finding that the effect of FD-iMPs was comparable with the original iMPs in animal models indicates that lyophilization contributes to the stability of iMPs and enables their long-term storage and transport.

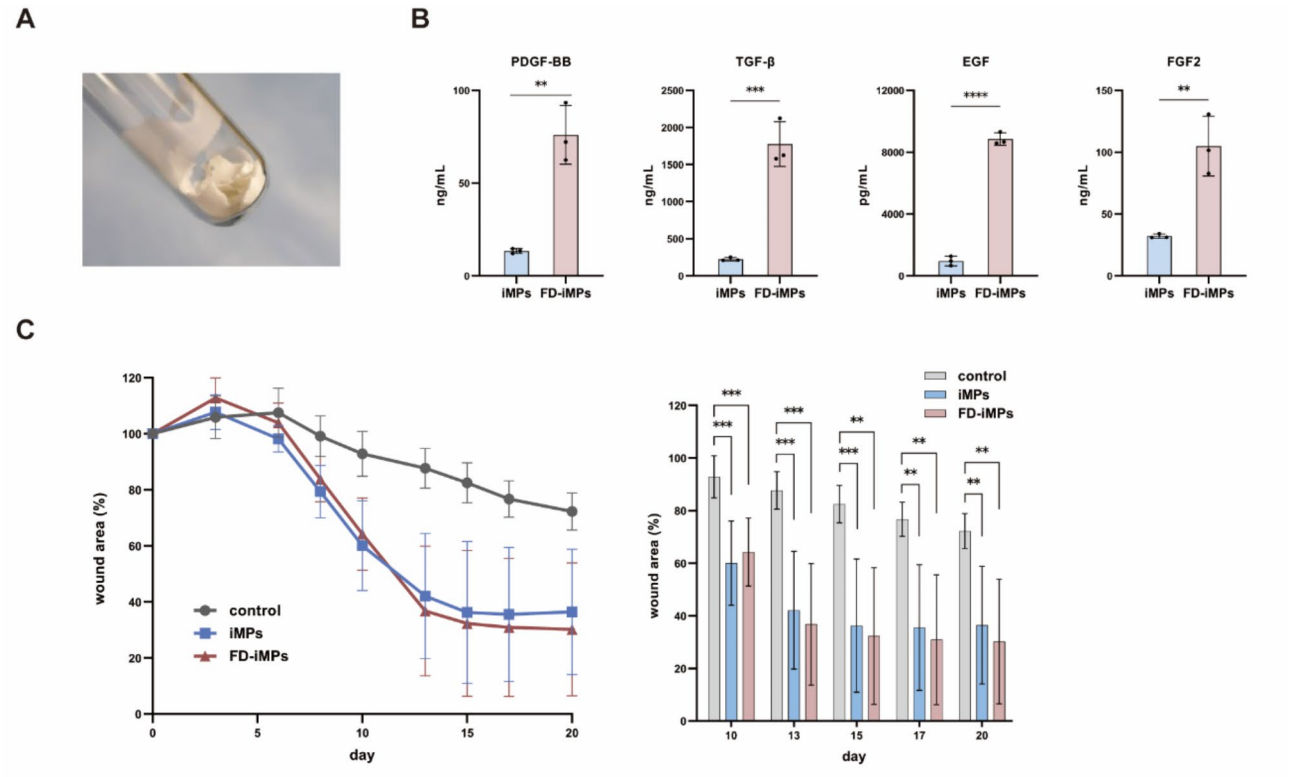


**Fig. 7** Validation of FD-iMPs. **A** Photograph of FD-iMPs in a test tube. iMPs were lyophilized and stored at 4 °C for 90 days. **B** Stability of growth factors in FD-iMPs. Following suspension in PBS to the same volume as before lyophilization, the concentration of growth factors in FD-iMPs was measured and compared to that in the original iMPs. $n = 3$. **C** Efficacy of FD-iMPs in the animal model. The in vivo wound healing assay was performed similarly as with the original iMPs described in Fig. 6. $n = 9$. Data are presented as the mean ± SD. ** $p < 0.01$, *** $p < 0.001$, **** $p < 0.0001$

This study has several limitations. First, the influence of iMPs on cells with a specific role in wound healing, such as keratinocytes and immune cells including neutrophils and macrophages, has not been explored. Second, there are some critical differences between our animal models and the chronic wounds in human patients. Whereas wound healing in human skin is proceeded by granulation, contraction is the primary mechanism in rodents [39]. In addition, the animal models in which treatment and analysis are initiated simultaneously with the preparation of skin injury do not replicate the inflammatory conditions caused by infection in chronic wounds. Finally, despite previous reports that platelet-derived extracellular vesicles [40] and mitochondria [41] promote wound healing, these factors were not investigated in this study. These issues need to be considered in future research.

## Conclusion

This study shows that iMPs promote wound healing through the activation of vascular endothelial cells and fibroblasts. FGF2 specifically detected in iMPs contributed to the proliferation of vascular endothelial cells. Furthermore, RNA-seq revealed that iMPs induce the polarity of stalk cells and upregulate *ANGPTL4* gene in vascular endothelial cells independent of FGF2 signaling. These mechanisms were suggested to provide the superior effects of iMPs on wound healing and angiogenesis compared to PRP. Finally, lyophilization ensured the stability of iMPs and enabled long-term storage. Overall, iMPs have potential for future clinical application as a treatment for chronic wounds.

### Abbreviations

| | |
|---|---|
| PRP | Platelet-rich plasma |
| iPSC | Induced pluripotent stem cell |
| iMPs | iPSC-derived megakaryocytes and platelets |
| HUVECs | Human umbilical vein endothelial cells |
| FD-iMPs | Freeze-dried iMPs |
| PDGF-BB | Platelet-derived growth factor-BB |
| FGF2 | Fibroblast growth factor 2 |
| VEGF | Vascular endothelial growth factor |
| imMKCLs | Immortalized megakaryocyte cell lines |
| IMDM | Iscove's modified Dulbecco medium |
| FBS | Fetal bovine serum |
| SCF | Stem cell factor |
| Dox | Doxycycline |
| PBS | Phosphate-buffered saline |
| PPP | Platelet-poor plasma |
| TGF-β | Transforming growth factor beta |
| EGF | Epidermal growth factor |
| IGF1 | Insulin-like growth factor 1 |
| ELISA | Enzyme-linked immuno sorbent assay |
| DMEM | Dulbecco's modified Eagle medium |
| DMSO | Dimethyl sulfoxide |
| RT-qPCR | Quantitative reverse transcription polymerase chain reaction |

## Supplementary Information

The online version contains supplementary material available at https://doi.org/10.1186/s13287-024-03966-z.

Supplementary Material 1

Supplementary Material 2

Supplementary Material 3

**Acknowledgements**
The authors would like to thank Peter Karagiannis for English language editing.

**Author contributions**
K.K. designed the study, the main conceptual ideas, and the proof outline. N.T. aided in interpreting the results and worked on the manuscript. S.K.P., M.F., B.R., and A.K. performed the RNA-seq. N.T., M.O., and A.I. analyzed the RNA seq data. M.A.K., I.T., and M.M. participated in the data collection. Y.K., S.A., and N.F. provided technical support and analyzed the data. N.M. and K.E. supervised the project. All the authors read and approved the final manuscript.

**Funding**
This work was supported by a grant-in-aid for scientific research (JP21K16921 to K.K., JP23K09095 to K.K. and 21H05047S to K.E.) from the Japan Society for the Promotion of Science (JSPS); by Terumo Life Science Foundation to K.E.; by Incubation Program of Kyoto University to K.E.; by SBC Medical Promotion Foundation to K.K.; by an unrestricted grant from Jiyugaoka Clinic Doctor's Cosmetics, Shin-kuki General Hospital and Shin-yurigaoka General Hospital to N.M. The funding bodies played no role in the design of the study, collection, analysis, and interpretation of the data, or writing of the manuscript.

**Data availability**
The RNA-sequencing data has been uploaded to NCBI's Gene Expression Omnibus (GEO) and can be accessed by the public (ID: GSE260954). All data generated or analyzed in this study are included in this article.

## Declarations

**Ethics approval and consent to participate**
This study was conducted according to the principles outlined in the Declaration of Helsinki and after receiving approval by the Ethics Committee of Chiba University (approval number: 1045, approval date: 20 February 2020, name of project: Clinical research for the development of artificial platelets with expanded function). All subjects provided informed written consent for the collection of samples and subsequent analysis. All animal experiments were approved by the Chiba University Institutional Animal Care and Use Committee (approval number: 5-158, approval date: 9 March 2023, name of project: Research for the development of artificial platelets with disease-specific therapeutic factors.).

**Consent for publication**
Not applicable.

**Competing interests**
K.K., N.T., M.M. and K.E. hold stock of Kineplat Co.Ltd. that has a related patent of this research.

**Author details**
[1]Department of Plastic, Reconstructive, and Aesthetic Surgery, Chiba University Graduate School of Medicine, Chiba, Japan
[2]Department of Regenerative Medicine, Chiba University Graduate School of Medicine, Chiba, Japan
[3]Division of Stem Cell and Molecular Medicine, Center for Stem Cell Biology and Regenerative Medicine, The Institute of Medical Science, The University of Tokyo, Tokyo, Japan
[4]Department of Molecular Oncology, Chiba University Graduate School of Medicine, Chiba, Japan
[5]Department of Orthopedic Surgery, Chiba University Graduate School of Medicine, Chiba, Japan
[6]Jiyugaoka Clinic, Tokyo, Japan
[7]Health and Disease Omics Center, Chiba University, Chiba, Japan
[8]Department of Clinical Application, Center for iPS Cell Research and Application (CiRA), Kyoto University, Kyoto, Japan

Received: 15 March 2024 / Accepted: 30 September 2024
Published online: 14 October 2024

**References**

1. Hopman WM, Harrison MB, Coo H, Friedberg E, Buchanan M, VanDenKerkhof EG. Associations between chronic disease, age and physical and mental health status. Chronic Dis Can. 2009;29(3):108–16.
2. Armstrong DG, Wrobel J, Robbins JM. Guest Editorial: are diabetes-related wounds and amputations worse than cancer? Int Wound J. 2007;4(4):286–7.
3. Sen CK, Gordillo GM, Roy S, Kirsner R, Lambert L, Hunt TK, et al. Human skin wounds: a major and snowballing threat to public health and the economy. Wound Repair Regen. 2009;17(6):763–71.
4. Wilkinson HN, Hardman MJ. Wound healing: cellular mechanisms and pathological outcomes. Open Biol. 2020;10(9):200223.
5. Smiell JM, Wieman TJ, Steed DL, Perry BH, Sampson AR, Schwab BH. Efficacy and safety of becaplermin (recombinant human platelet-derived growth factor-BB) in patients with nonhealing, lower extremity diabetic ulcers: a combined analysis of four randomized studies. Wound Repair Regen. 1999;7(5):335–46.
6. Richard JL, Parer-Richard C, Daures JP, Clouet S, Vannereau D, Bringer J, et al. Effect of topical basic fibroblast growth factor on the healing of chronic diabetic neuropathic ulcer of the foot. A pilot, randomized, double-blind, placebo-controlled study. Diabetes Care. 1995;18(1):64–9.
7. Hanft JR, Pollak RA, Barbul A, van Gils C, Kwon PS, Gray SM, et al. Phase I trial on the safety of topical rhVEGF on chronic neuropathic diabetic foot ulcers. J Wound Care. 2008;17(1):30–2. 4–7.
8. Han G, Ceilley R. Chronic Wound Healing: a review of current management and treatments. Adv Ther. 2017;34(3):599–610.
9. Eppley BL, Woodell JE, Higgins J. Platelet quantification and growth factor analysis from platelet-rich plasma: implications for wound healing. Plast Reconstr Surg. 2004;114(6):1502–8.
10. Taniguchi Y, Yoshioka T, Sugaya H, Gosho M, Aoto K, Kanamori A, et al. Growth factor levels in leukocyte-poor platelet-rich plasma and correlations with donor age, gender, and platelets in the Japanese population. J Exp Orthop. 2019;6(1):4.
11. Yuan Z, Wang Y, Li Y, Lin C, Wang S, Wang J, et al. Comparison of Leukocyte-Rich and Leukocyte-Poor platelet-rich plasma on pressure Ulcer in a rat model. J Burn Care Res. 2023;44(4):860–8.
12. Assirelli E, Filardo G, Mariani E, Kon E, Roffi A, Vaccaro F, et al. Effect of two different preparations of platelet-rich plasma on synoviocytes. Knee Surg Sports Traumatol Arthrosc. 2015;23(9):2690–703.
13. Jain NK, Gulati M. Platelet-rich plasma: a healing virtuoso. Blood Res. 2016;51(1):3–5.
14. Takayama N, Nishimura S, Nakamura S, Shimizu T, Ohnishi R, Endo H, et al. Transient activation of c-MYC expression is critical for efficient platelet generation from human induced pluripotent stem cells. J Exp Med. 2010;207(13):2817–30.
15. Nakamura S, Takayama N, Hirata S, Seo H, Endo H, Ochi K, et al. Expandable megakaryocyte cell lines enable clinically applicable generation of platelets from human induced pluripotent stem cells. Cell Stem Cell. 2014;14(4):535–48.
16. Ito Y, Nakamura S, Sugimoto N, Shigemori T, Kato Y, Ohno M, et al. Turbulence activates platelet Biogenesis to Enable Clinical Scale Ex vivo production. Cell. 2018;174(3):636–e4818.
17. Huber SC, Junior J, Silva LQ, Montalvão SAL, Annichino-Bizzacchi JM. Freeze-dried versus fresh platelet-rich plasma in acute wound healing of an animal model. Regen Med. 2019;14(6):525–34.
18. Shimasaki T, Yamamoto S, Omura R, Ito K, Nishide Y, Yamada H et al. Novel platform for regulation of Extracellular vesicles and metabolites secretion from cells using a multi-linkable horizontal co-culture plate. Micromachines (Basel). 2021;12(11).
19. Takayama N, Murison A, Takayanagi SI, Arlidge C, Zhou S, Garcia-Prat L, et al. The transition from quiescent to activated States in Human hematopoietic stem cells is governed by dynamic 3D genome reorganization. Cell Stem Cell. 2021;28(3):488–e50110.

20. Barrientos S, Stojadinovic O, Golinko MS, Brem H, Tomic-Canic M. Growth factors and cytokines in wound healing. Wound Repair Regen. 2008;16(5):585–601.
21. Garoufalia Z, Papadopetraki A, Karatza E, Vardakostas D, Philippou A, Kouraklis G, et al. Insulin-like growth factor-I and wound healing, a potential answer to non-healing wounds: a systematic review of the literature and future perspectives. Biomed Rep. 2021;15(2):66.
22. Hinz B, Phan SH, Thannickal VJ, Prunotto M, Desmoulière A, Varga J, et al. Recent developments in myofibroblast biology: paradigms for connective tissue remodeling. Am J Pathol. 2012;180(4):1340–55.
23. Cialdai F, Risaliti C, Monici M. Role of fibroblasts in wound healing and tissue remodeling on Earth and in space. Front Bioeng Biotechnol. 2022;10:958381.
24. Sedlář A, Trávníčková M, Matějka R, Pražák Š, Mészáros Z, Bojarová P et al. Growth factors VEGF-A(165) and FGF-2 as multifunctional biomolecules governing cell adhesion and proliferation. Int J Mol Sci. 2021;22(4).
25. Liu PCC, Koblish H, Wu L, Bowman K, Diamond S, DiMatteo D, et al. INCB054828 (pemigatinib), a potent and selective inhibitor of fibroblast growth factor receptors 1, 2, and 3, displays activity against genetically defined tumor models. PLoS ONE. 2020;15(4):e0231877.
26. Sootome H, Fujita H, Ito K, Ochiiwa H, Fujioka Y, Ito K, et al. Futibatinib is a novel irreversible FGFR 1–4 inhibitor that shows selective Antitumor activity against FGFR-Deregulated tumors. Cancer Res. 2020;80(22):4986–97.
27. Kolberg L, Raudvere U, Kuzmin I, Adler P, Vilo J, Peterson H. G:profiler-interoperable web service for functional enrichment analysis and gene identifier mapping (2023 update). Nucleic Acids Res. 2023;51(W1):W207–12.
28. De Smet F, Segura I, De Bock K, Hohensinner PJ, Carmeliet P. Mechanisms of vessel branching: filopodia on endothelial tip cells lead the way. Arterioscler Thromb Vasc Biol. 2009;29(5):639–49.
29. Chen W, Xia P, Wang H, Tu J, Liang X, Zhang X, et al. The endothelial tip-stalk cell selection and shuffling during angiogenesis. J Cell Commun Signal. 2019;13(3):291–301.
30. Chaube B, Citrin KM, Sahraei M, Singh AK, de Urturi DS, Ding W, et al. Suppression of angiopoietin-like 4 reprograms endothelial cell metabolism and inhibits angiogenesis. Nat Commun. 2023;14(1):8251.
31. Armstrong DG, Tan TW, Boulton AJM, Bus SA. Diabetic Foot Ulcers: a review. JAMA. 2023;330(1):62–75.
32. Marx RE, Carlson ER, Eichstaedt RM, Schimmele SR, Strauss JE, Georgeff KR. Platelet-rich plasma: growth factor enhancement for bone grafts. Oral Surg Oral Med Oral Pathol Oral Radiol Endod. 1998;85(6):638–46.
33. Meznerics FA, Fehérvári P, Dembrovszky F, Kovács KD, Kemény LV, Csupor D, et al. Platelet-Rich plasma in Chronic Wound Management: a systematic review and Meta-analysis of Randomized clinical trials. J Clin Med. 2022;11:24.
34. Ochi K, Takayama N, Hirose S, Nakahata T, Nakauchi H, Eto K. Multicolor staining of globin subtypes reveals impaired globin switching during erythropoiesis in human pluripotent stem cells. Stem Cells Transl Med. 2014;3(7):792–800.
35. Liu Y, Liu Y, Deng J, Li W, Nie X. Fibroblast growth factor in Diabetic Foot Ulcer: progress and therapeutic prospects. Front Endocrinol (Lausanne). 2021;12:744868.
36. Chen H, Charlat O, Tartaglia LA, Woolf EA, Weng X, Ellis SJ, et al. Evidence that the diabetes gene encodes the leptin receptor: identification of a mutation in the leptin receptor gene in db/db mice. Cell. 1996;84(3):491–5.
37. Li G, Ko CN, Li D, Yang C, Wang W, Yang GJ, et al. A small molecule HIF-1α stabilizer that accelerates diabetic wound healing. Nat Commun. 2021;12(1):3363.
38. Mukai K, Horike SI, Meguro-Horike M, Nakajima Y, Iswara A, Nakatani T. Topical estrogen application promotes cutaneous wound healing in db/db female mice with type 2 diabetes. PLoS ONE. 2022;17(3):e0264572.
39. Zomer HD, Trentin AG. Skin wound healing in humans and mice: challenges in translational research. J Dermatol Sci. 2018;90(1):3–12.
40. Guo SC, Tao SC, Yin WJ, Qi X, Yuan T, Zhang CQ. Exosomes derived from platelet-rich plasma promote the re-epithelization of chronic cutaneous wounds via activation of YAP in a diabetic rat model. Theranostics. 2017;7(1):81–96.
41. Jin P, Pan Q, Lin Y, Dong Y, Zhu J, Liu T, et al. Platelets facilitate Wound Healing by mitochondrial transfer and reducing oxidative stress in endothelial cells. Oxid Med Cell Longev. 2023;2023:2345279.


## Publisher's note